Supporting information for:

Exploration of the interaction between dynein intermediate chain and dynactin p150^{Glued} reveals a novel binding interface

AJ Di Nicola, Bryn L. Romig, Stella M. Davis, Paul H. Cleary, Claire H. Yung, Daniel R. Marsan, Anna C. Merkt, Nikolaus M. Loening*

Department of Chemistry, Lewis & Clark College, 615 S Palatine Hill Road, Portland, OR 97219, United States

*Corresponding Author. Email: loening@lclark.edu

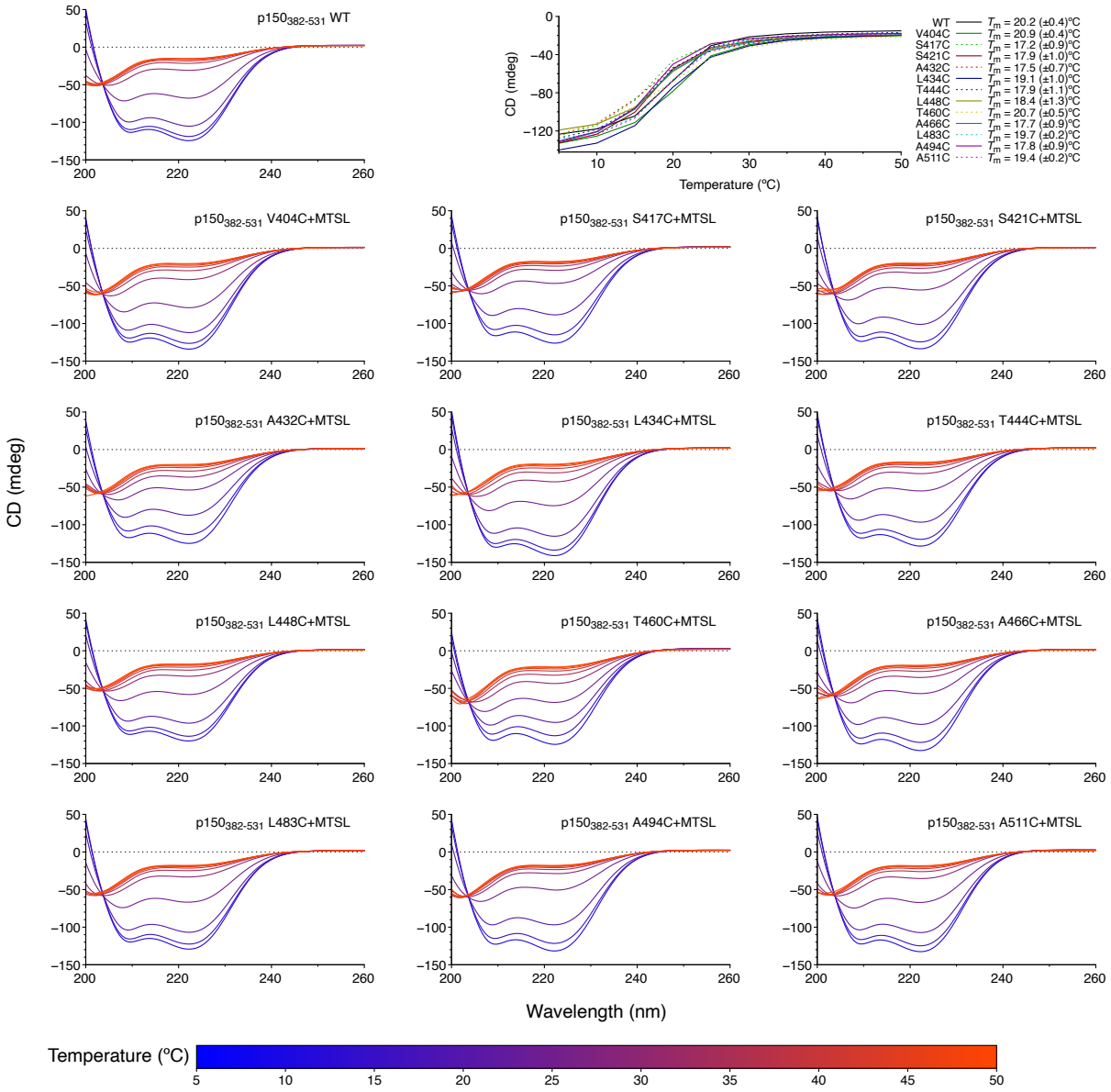

Figure S1. Single-cysteine mutations and MTSL labeling do not significantly impact the coiled-coiled structure of p150$_{382\text{-}531}$. CD spectra of p150$_{382\text{-}531}$ WT (top left) are almost identical to the CD spectra for single-cysteine p150$_{382\text{-}531}$ mutants after MTSL labeling. Small variations in the magnitude of the CD signal are due to small variations in the sample concentration; all samples were at ≈18 μM in 150 mM sodium chloride/50 mM sodium phosphate (pH 7.4). CD spectra were collected at 5-degree intervals from 5 to 50°C. Data shown in the graph at top right are the average mean ellipticity (mdeg) from 220 to 224 nm for each sample at each temperature. The denaturation midpoint temperatures (T_m) were estimated by fitting the data to a two-site (N ⇌ D) model using CDpal [1].

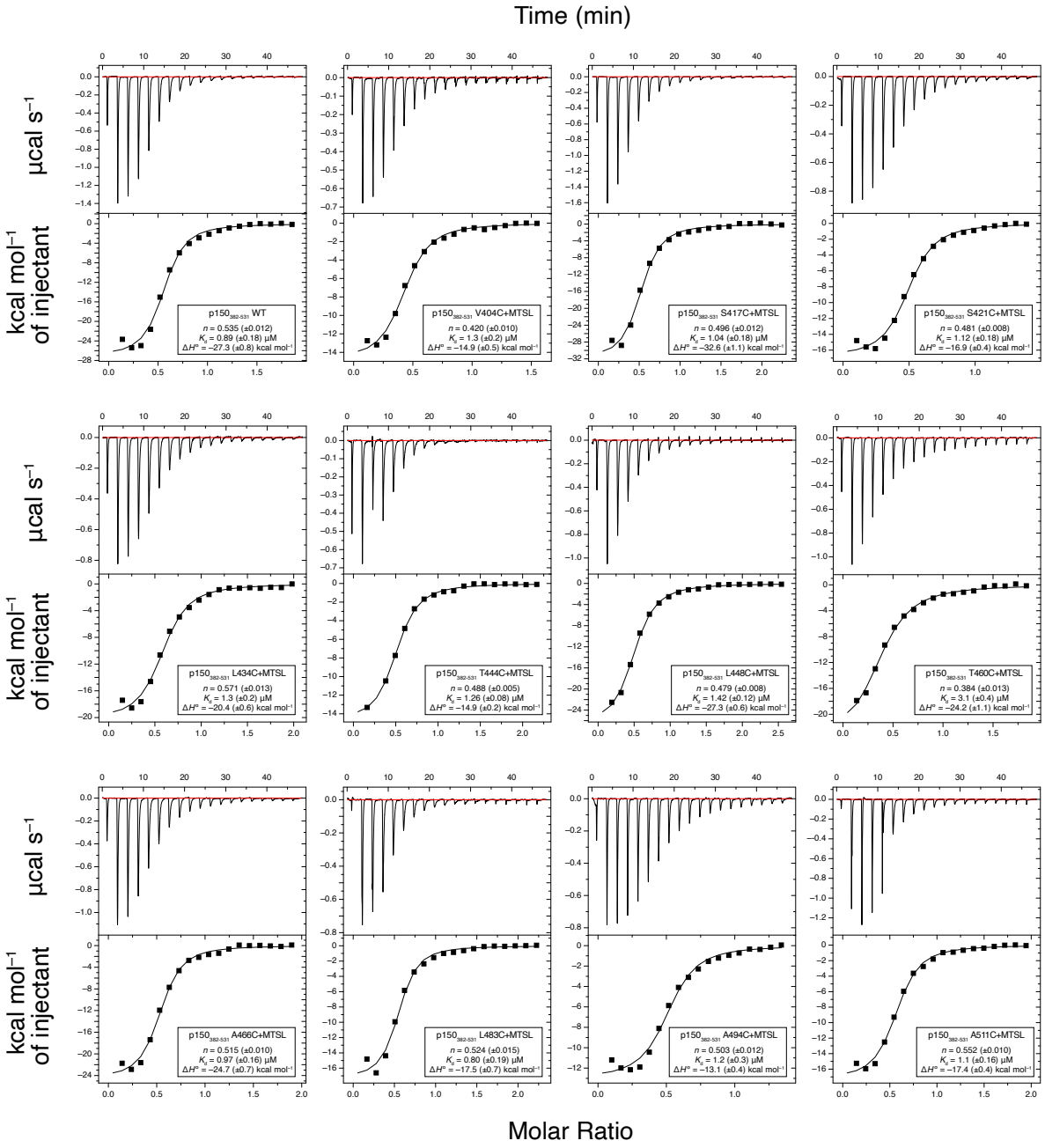

Figure S2. ITC shows that wild-type p150$_{382\text{-}531}$ and MTSL-labeled single-cysteine p150$_{382\text{-}531}$ mutants bind similarly to IC-2C$_{1\text{-}96}$. Shown are representative ITC thermograms (top) and binding isotherms (bottom) for titrations of 350-400 µM IC-2C$_{1\text{-}96}$ in the syringe with 25-55 µM p150$_{382\text{-}531}$ in the sample cell. All ITC runs were carried out at 15ºC and typically resulted in values of $n \sim 0.5$, $K_d \sim 1$ µM, and $\Delta H \sim -25$ kcal mol^{-1}. The numerical results shown are from fitting these single runs to a one set of sites model using Origin 7.0. The errors provided for the parameters are the fit errors, which will typically underestimate the actual errors (which are mainly due to uncertainties in the concentration measurements and batch-to-batch variations in sample quality).

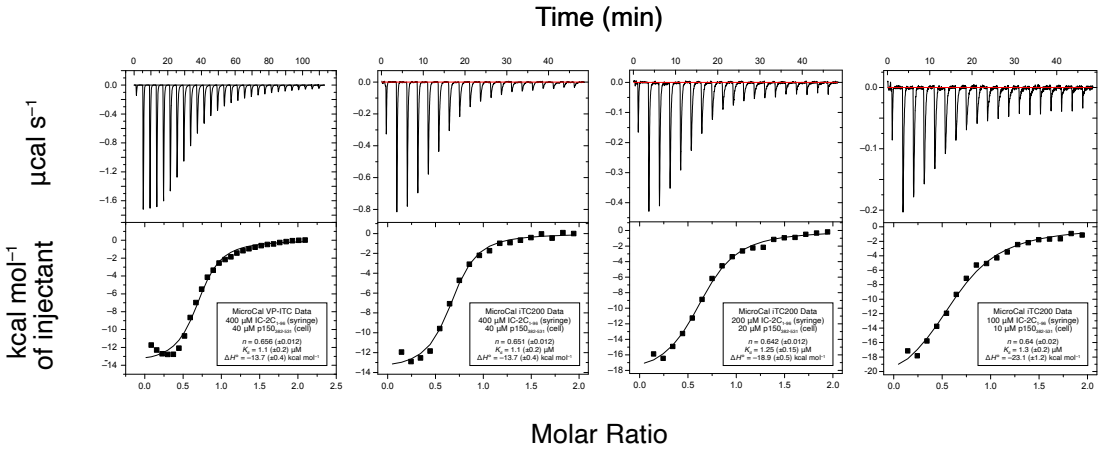

Figure S3. The binding affinity of p150$_{382-531}$ to IC-2C$_{1-96}$ does not vary with concentration. Thermograms (top) and binding isotherms (bottom) from ITC titrations at 15ºC of IC-2C$_{1-96}$ in the syringe with p150$_{382-531}$ in the cell. Concentrations used were 400 µM IC-2C$_{1-96}$ with 40 µM p150$_{382-531}$ (far left, center left), 200 µM IC-2C$_{1-96}$ with 20 µM p150$_{382-531}$ (center right) and 100 µM IC-2C$_{1-96}$ with 10 µM p150$_{382-531}$ (far right). All thermograms were acquired using the same batches of IC-2C$_{1-96}$ and p150$_{382-531}$. The numerical results shown are from fitting these single runs to a one set of sites model using Origin 7.0. The errors provided for the parameters are the fit errors, which will typically underestimate the actual errors (which are mainly due to uncertainties in the concentration measurements and batch-to-batch variations in sample quality). The thermogram shown at far left was acquired with a MicroCal VP-ITC system, whereas the other thermograms were acquired using a MicroCal iTC200 system.

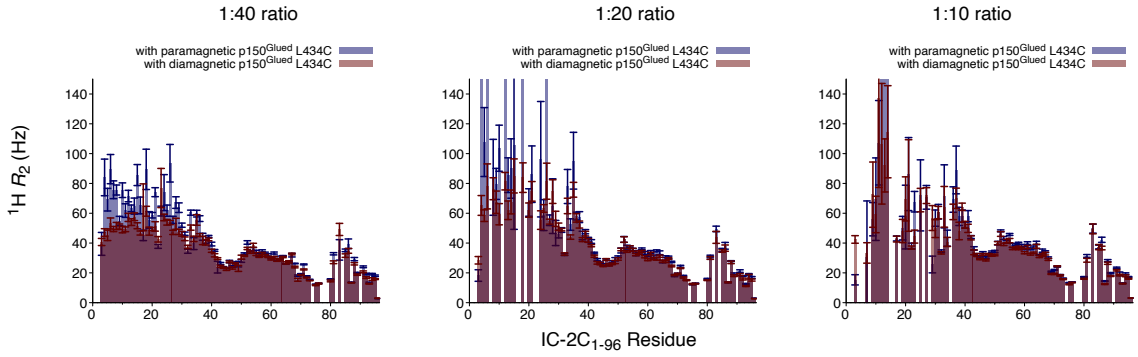

Figure S4. A 1:40 ratio of MTSL-labeled p150$_{382-531}$ L434C to ^{15}N-labeled IC-2C$_{1-96}$ allows for the more accurate determination of paramagnetic relaxation enhancements (PREs). Amide proton R_2 values were measured for ^{15}N-labeled IC-2C$_{1-96}$ before (paramagnetic, blue) and after (diamagnetic, red) reduction of MTSL-labeled p150$_{382-531}$ L434C. The L434C mutant was used as we know it has a strong PRE effect on the SAH region. The difference in the relaxation rates (paramagnetic vs. diamagnetic) is the PRE. The ratio of MTSL-labeled p150$_{382-531}$ L434C to ^{15}N-labeled IC-2C$_{1-96}$ was 1:40 (15 µM to 600 µM, shown on left), 1:20 (30 µM to 600 µM, shown in center), and 1:10 (60 µM to 600 µM, shown on right). Gaps in the data are due to prolines (residues 74, 77, 78, 79, 82, 90) or where peak overlap and/or attenuation prevented accurate data analysis. The 1:40 ratio resulted in data from all residues in the SAH region, whereas other ratios resulted in the peaks from some residues being so attenuated that they could not be measured. In addition, the data for the 1:40 ratio had the smallest errors for the relaxation rates; the errors were determined by fitting the data to an exponential decay model using CCPN Analysis 2.5.2 [2].

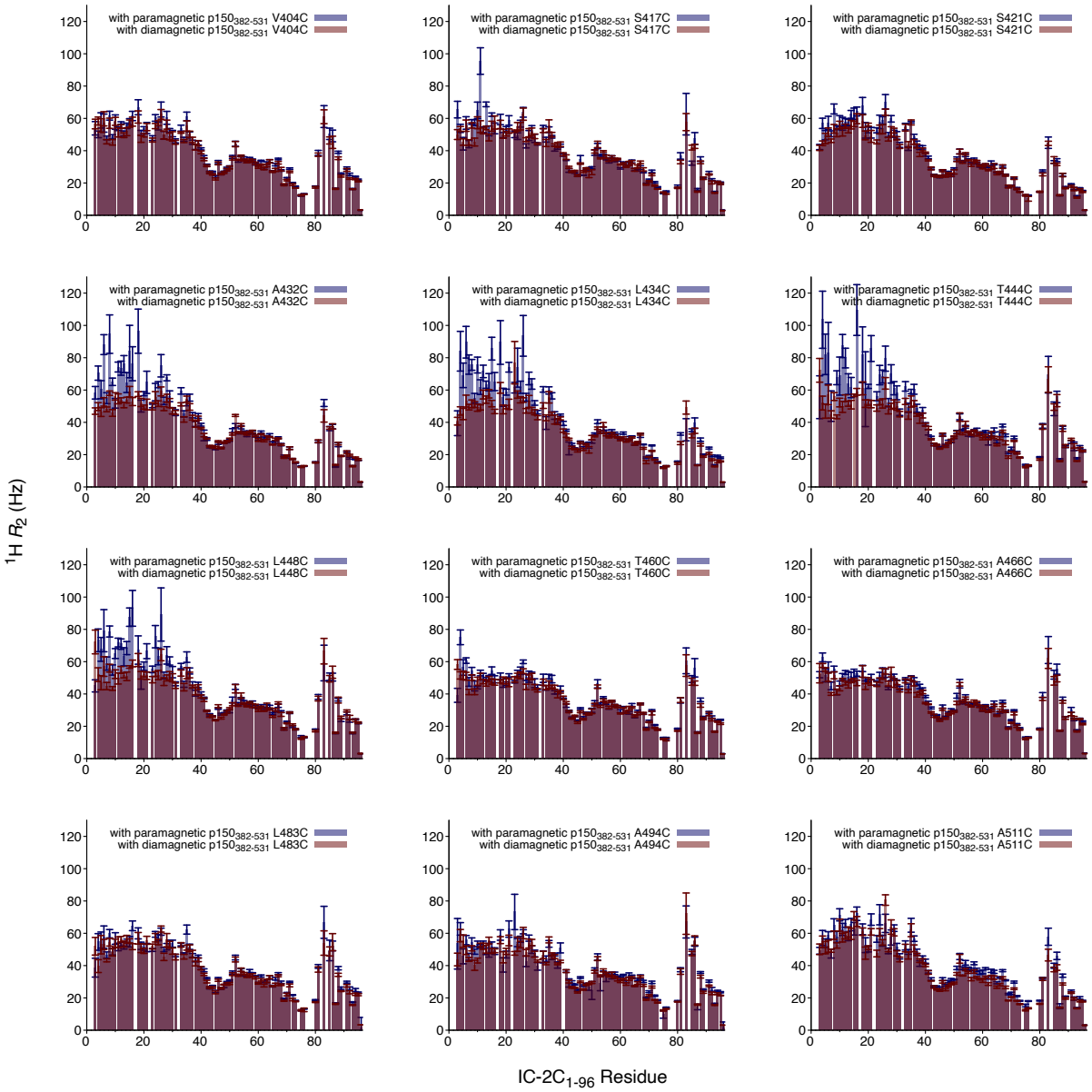

Figure S5. The largest changes in the rate of proton transverse relaxation (^{1}H R_2) for amide residues in the single α-helix (SAH) region of IC-2C$_{1\text{-}96}$ occurred when the MTSL label on p150$_{382\text{-}531}$ was attached to residues 432, 434, 444, and 448. Amide proton R_2 values were measured for 600 μM ^{15}N-labeled IC-2C$_{1\text{-}96}$ before (paramagnetic, blue) and after (diamagnetic, red) reduction of 15 μM MTSL-labeled single-cysteine mutants of p150$_{382\text{-}531}$. The difference in the relaxation rates (paramagnetic vs. diamagnetic) is the PRE. Gaps in the data are due to prolines (residues 74, 77, 78, 79, 82, 90) or where peak overlap and/or attenuation prevented accurate data analysis. Error bars are based on the error for the relaxation rates determined by fitting the data to an exponential decay model using CCPN Analysis 2.5.2 [2].

Derivation of Equation 2:

For a protein with an average number of tryptophans and tyrosines, the ratio of the molar absorptivities at 205 and 280 nm is approximately 30 [3]. For proteins that do not have an average number of tyrosines and tryptophans (i.e., proteins the absorb unusually strongly or unusually weakly at 280 nm compared to an "average protein"), the difference in absorbance at 205 and 280 nm can be used to correct for the presence of contaminant proteins if we can assume that the contaminants behave like "average" proteins:

$$\varepsilon_{205,\text{contaminant}} = 30 \times \varepsilon_{280,\text{contaminant}}$$

With this assumption, we can set up two equations (for A_{205} and A_{280}) with two unknowns (the concentrations of the target protein and the contaminants):

$$A_{205} = \varepsilon_{205,\text{protein}}[\text{protein}] + \underbrace{\varepsilon_{205,\text{contaminant}}}_{=30\times\varepsilon_{280,\text{contaminant}}}[\text{contaminant}]$$

$$A_{280} = \varepsilon_{280,\text{protein}}[\text{protein}] + \varepsilon_{280,\text{contaminant}}[\text{contaminant}]$$

Multiplying the second equation by 30 and then subtracting it from the first equation, the terms having to do with the concentration of the contaminant cancel out:

$$A_{205} - 30 \times A_{280} = \varepsilon_{205,\text{protein}}[\text{protein}] - 30 \times \varepsilon_{280,\text{protein}}[\text{protein}]$$

which can be rearranged to yield the following equation (Equation 2 in the main text):

$$[\text{protein}] = \frac{A_{205} - (30 \times A_{280})}{\varepsilon_{205,\text{protein}} - (30 \times \varepsilon_{280,\text{protein}})} \quad (2)$$

Equation 2 should only be used for proteins that absorb unusually weakly at 280 nm (as is the case with many intrinsically disordered proteins, which are typically deficient in aromatic amino acids). Although in theory it can also be used for proteins that absorb abnormally strongly at 280 nm, it would be exceedingly rare for a protein to have such an excess of tryptophans and tyrosines as to make using this equation worthwhile. This equation should not be used for target proteins that have close to an "average" number of tyrosines and tryptophans, as the closer the target protein is to fulfilling the condition $\varepsilon_{205,\text{protein}}/\varepsilon_{280,\text{protein}} = 30$, the more that errors in the absorbance measurements, errors in the estimated molar absorptivities, and errors due to the assumption of the factor of 30 for contaminant proteins will be magnified in the "corrected" concentration. For $p150_{382\text{-}531}$, $\varepsilon_{205,\text{protein}}/\varepsilon_{280,\text{protein}} > 150$, so we can comfortably use Equation 2.

This correction works best for a target protein without any tyrosines and tryptophans (such as IC-$2C_{1\text{-}96}$), in which case $\varepsilon_{280,\text{protein}} = 0$ and Equation 2 reduces to:

$$[\text{protein}] = \frac{A_{205} - (30 \times A_{280})}{\varepsilon_{205,\text{protein}}} \quad (3)$$

If the sample is completely pure, then the A_{280} should be zero, and the equation will produce the exact same results as a typical A_{205}-based concentration measurement.

References

[1] M. Niklasson, C. Andresen, S. Helander, M.G.L. Roth, A. Zimdahl Kahlin, M. Lindqvist Appell, L.-G. Mårtensson, P. Lundström, Robust and convenient analysis of protein thermal and chemical stability, Protein Sci 24 (2015) 2055–2062. https://doi.org/10.1002/pro.2809.

[2] W.F. Vranken, W. Boucher, T.J. Stevens, R.H. Fogh, A. Pajon, M. Llinas, E.L. Ulrich, J.L. Markley, J. Ionides, E.D. Laue, The CCPN data model for NMR spectroscopy: development of a software pipeline, Proteins 59 (2005) 687–696. https://doi.org/10.1002/prot.20449.

[3] N.J. Anthis, G.M. Clore, Sequence-specific determination of protein and peptide concentrations by absorbance at 205 nm, Protein Sci 22 (2013) 851–858. https://doi.org/10.1002/pro.2253.